

# Compositionally Driven Viscometric Behaviors of Poly (Alkyl Methacrylates) in Lubricating Oils

Reid A. Patterson\*, Christopher P. Kabb, David M. Nickerson\*, Eugene Pashkovski

Research and Development, The Lubrizol Corporation, Wickliffe, USA

Email: \*reid.patterson@lubrizol.com, \*david.nickerson@lubrizol.com

**How to cite this paper:** Patterson, R.A., Kabb, C.P., Nickerson, D.M. and Pashkovski, E. (2022) Compositionally Driven Viscometric Behaviors of Poly (Alkyl Methacrylates) in Lubricating Oils. *Advances in Chemical Engineering and Science*, 12, 65-86.

<https://doi.org/10.4236/aces.2022.122006>

**Received:** January 20, 2022

**Accepted:** March 20, 2022

**Published:** March 23, 2022

Copyright © 2022 by author(s) and Scientific Research Publishing Inc. This work is licensed under the Creative Commons Attribution International License (CC BY 4.0).

<http://creativecommons.org/licenses/by/4.0/>



Open Access

## Abstract

Viscosity index (VI) and shear stability index (SSI) are standard methods used in the lubricant industry to determine temperature-viscosity dependency and resistance to product degradation, respectively. A variety of oil-soluble polymers, including poly(alkyl methacrylates) (PAMAs) are routinely used to control these properties in fully-formulated liquid lubricants. In this report, we use reversible addition-fragmentation chain transfer (RAFT) polymerization to precisely target identical degrees of polymerization in a family of PAMAs with varying lauryl, hexyl, butyl, ethyl, and methyl groups. Then, expanding on previous methodology reported in the literature, we establish structure property relationships for these PAMAs, specifically looking at how intrinsic viscosity  $[\eta]$  and Martin interaction parameters  $K_M$  relate to VI and SSI characteristics. While the intrinsic viscosity  $[\eta]$  is associated with the volume of macromolecules at infinite dilution, the parameter  $K_M$  reflects the hydrodynamic interactions of polymer chains at actual polymer concentrations in lubricating oils. In this paper, we show that the dependence of VI on the non-dimensional concentration  $c/c^*$  (or  $c[\eta]$ ) can be presented in a form of master curve with shift factors proportional to  $K_M$  that decreases with increasing size of alkyl groups. This finding implies that even in the dilute regime, the coil-expansion theory used to explain the effect of macromolecules on VI should be complemented with the idea of hydrodynamic interactions between polymer molecules that can be controlled by the choice of alkyl chains in the family of PAMAs.

## Keywords

Viscosity Index, Shear Stability Index, Polymethacrylates, Lubricating Oils

## 1. Introduction

A powerful and widely-applied strategy for reducing frictional losses between two moving mating surfaces is to separate the surfaces by means of lubricating oil. In this way, frictional penalties due to solid-to-solid contacts are greatly reduced by hydrodynamic lubrication [1] [2]. To maintain the load-bearing characteristics which lead to this fluid film, the lubricant must maintain a minimum viscosity across its entire range of operating conditions, including those occurring at high temperatures and high shear environments. While these minimum viscosity requirements at higher operating temperatures are critical for maintaining durability and efficiency, at lower operating temperature regimes, the natural increase in the lubricant's viscosity is counterproductive to overall operational efficiency. One strategy then, to improve overall efficiency, has been to use lubricants that have been designed to have weak viscosity-temperature dependence and a reduced average viscosity across their entire operational temperature range. This reduced average viscosity has been shown to be an effective formulation strategy for the improvement of overall operational efficiencies in automotive and industrial lubricant applications [3] [4] [5] [6].

Within the automotive and industrial lubrication field, one of the most widely used metrics for assessing a lubricant's viscosity-temperature dependence is the viscosity index (VI), determined by comparing a fluid's kinematic viscosity at 40°C to that of a known reference fluid with identical kinematic viscosity at 100°C. Fluids with higher viscosity indices have reduced viscosity-temperature dependence. A highly impactful strategy to impart increased viscosity index to a lubricating oil is by the addition of soluble polymer components known as viscosity index improvers (VII). The general nature of these polymers is known to have a significant impact on the VI contribution, and previous research has used coil-expansion theory to provide mechanistic insights into how VII's impart increased VI [7] [8] [9] [10]. These previous investigations have largely sought to describe the VI impact of polymers treated at levels well below the theoretical overlap concentration. In higher treat applications, an interesting reversal of the VI impact is observed with certain types of VIIs wherein additional polymer content results in decreases to the viscosity index. Developing a more complete understanding of the mechanistic behaviors that lead to this reversal as well as what implications this behavior might have to other fundamental properties such as shear stability is the primary aim of this work.

### Coil-Expansion Theory and Recent Work

Coil-expansion theory has a long history in polymer research with two encompassing methods accounting for polymer expansion: continuous variation and discrete step. The continuous variation theory describes a scenario where polymer size scales by some proportionality with temperature [11] [12]. Alternatively, a discrete step-change in polymer size has also been observed, where the polymer radius of gyration or other measure of its size remains constant until a

significant step-change to the coil size is induced by a factor such as temperature, solubility, or concentration [13] [14].

For many decades, the Selby coil-expansion concept was the dominating theory on polymer behavior in lubricating oils, relating expansion to parameters such as VI [7]. Selby describes the complexity involved with comparing polymer dynamics and viscosity index as originally defined by Dean and Davis [8] as the practice for determining viscosity-temperature relationships [9]. Therein, the expansion of hydrodynamic volume with improved solvency and increasing temperature was described. This has since taken hold as the mechanism of choice used to describe polymer systems in commercial lubricating oils.

Although the coil-expansion model has typically been used to rationalize VI improvements, it must be noted that not all polymers follow this model. Specifically, significant differences are observed between the solution behavior of poly(alkyl methacrylates) (PAMAs) and polyisobutylene (PIB) [15] [16] [17] [18] [19]. In a recent contribution to the conversation, Covitch and Trickett verified that PAMAs follow the coil-expansion theory, but other polymers, such as ethylene-propylene copolymers (olefin copolymers, or OCPs), did not behave in the same manner [10]. In addition to determining intrinsic viscosity in mineral oil, they used small-angle neutron scattering (SANS) as a tool to measure the radius of gyration of macromolecules in various deuterated solvents at different temperatures and concentration regimes. Their work showed that the presence of slightly collapsing polymer chains can still lead to VI improvement. In contrast to the temperature-dependent increase in radius of gyration measured for PAMAs, it was shown that OCPs decreased in size at elevated temperature, but nonetheless had a positive VI effect. Ultimately, their work concludes that the Selby coil-expansion mechanism does not explain behavior in mineral oils for all polymer types.

Ramasamy, *et al.* [20] used molecular modeling (Large Atomic/Molecular Massively Parallel Simulation, or LAMMPS) to further confirm Covitch's conclusions that PAMAs followed the coil-expansion theory and OCPs did not. Here, they suggested that the oxygen present in the PAMA was the contributing factor in the coil expansion. The OCP, which does not contain oxygen, does not expand with heating. In simulations of a PAMA and a theoretical "oxygen-free" PAMA, they observed a temperature-dependent increase in coil size in the PAMA, in contrast to coil contraction in the oxygen-free model.

Willett, *et al.* [21] examined the VI phenomenon in additional chemistries to those referenced above. This work included polybutene in addition to PAMA and OCP and identified four cases for VI trends with concentration: Case 1—VI increases with concentration, linear or non-linear; Case 2—VI increases then plateaus or decreases; Case 3—VI does not increase or decrease; Case 4—VI decreases. Their analysis attributed many of these behaviors to expansion, contraction, interaction, and combinations of such.

It is clear from recent works that a coil-expansion theory may not fully describe VI effects for all polymer systems. This theory is based on isolated coil

solution behavior and does not consider the inter-chain hydrodynamic interactions occurring in engine oils. These interactions are quite significant at the concentration regimes encountered in liquid lubricants. Therefore, more detailed account for both, coil expansion and inter-molecular interactions is needed to aid in formulating engine oils with desirable viscosity index. In the work presented herein, we will discuss the contribution of coil volume and hydrodynamic interactions to viscosity of dilute and semi-dilute solutions of a well-defined family of PAMAs.

## 2. Experimental Section

### 2.1. Materials

All chemicals were used as received unless otherwise noted. Lauryl methacrylate, methyl methacrylate, butyl methacrylate, and butyl-2-methyl-2-[(dodecylsulfanylthiocarbonyl)sulfanyl] propionate (CTA-Ester) were sourced from The Lubrizol Corporation. Ethyl methacrylate (>98%) and hexyl methacrylate were purchased from VWR. A 3 cSt, Group III base oil under the trade name “Ultra-S3” was sourced from Phillips 66.

### 2.2. Polymer Synthesis

To study solely the effects of polymer solubility on VI and SSI, PAMAs with the same degree of polymerization (DP) and varying compositions were targeted. Conventional free radical polymerization (or use of a thiol chain transfer agent) is typically used to synthesize PAMAs, which does not allow for precise targeting of a specific polymer chain length. The inclusion of a suitable chain transfer agent, such as a thiocarbonylthio compound typically used in reversible addition-fragmentation chain transfer (RAFT) polymerization, provides significant control over the polymer composition [22]. Therefore, butyl-2-methyl-2-[(dodecylsulfanylthiocarbonyl)sulfanyl] propionate (CTA) was used to mediate the polymerizations. The five copolymers prepared were a poly(lauryl methacrylate) homopolymer (LMA), poly(hexyl methacrylate-*co*-lauryl methacrylate) copolymer (HMA:LMA), poly(butyl methacrylate-*co*-lauryl methacrylate) copolymer (BMA:LMA), poly(ethyl methacrylate-*co*-lauryl methacrylate) copolymer (EMA:LMA), and poly(methyl methacrylate-*co*-lauryl methacrylate) copolymer (MMA:LMA). In all polymerizations, the same degree of polymerization was targeted by employing a ratio of [monomer]:[CTA] of 100:1, and the comonomer compositions were set by the initial molar ratio of comonomers in the reaction (*i.e.*, 52:48 LMA:comonomer).

A generalized reaction procedure is as follows: Ultra-S3 base oil and butyl-2-methyl-2-[(dodecylsulfanylthiocarbonyl)sulfanyl] propionate (CTA-Ester) were added to a 2 L, 4-neck round bottom flask equipped with a glass stir rod, Claisen adapter with condenser and feeding tube inlet, a thermocouple and heating mantle, and a nitrogen inlet. Lauryl methacrylate, comonomer (optional), Ultra-S3 base oil, and *tert*-butyl peroxy-2-ethylhexanoate were added to a glass jar

and thoroughly mixed. The flask was heated to 100°C and the monomer/initiator mixture was added dropwise over approximately 90 min. The temperature was allowed to drop to 82.5°C and the reaction was held at temperature until the monomer conversion was complete. After polymerization, the polymers were diluted to constant oil (50 wt%) and the molecular weights were analyzed by gel permeation chromatography (GPC, Supplementary **Figure S1**). These results are shown in **Table 1**.

The values of statistical coil size were calculated using relation  $\langle R^2 \rangle = C_{\infty}nl^2$  where  $n = 200$  is the number of bonds per chain and  $l = 0.15$  nm is the bond length [11]. Introducing comonomers with shorter alkyl chains (*e.g.*, butyl, ethyl, or methyl) makes chains more flexible so that the chain volume of LMA is approximately 1.4 times greater than these copolymers. However, inclusion of hexyl methacrylate in the copolymer results in a characteristic ratio much closer to that of LMA homopolymer.

### 2.3. Blending

Polymer samples (at 50 wt% in Ultra-S3 base oil) were added to a jar and diluted with the appropriate amount of Ultra-S3 base oil (final sample wt% ranged from 1 wt% to 25 wt% polymer). The mixture was heated to 70°C and stirred for 1 h until the sample was homogenous.

### 2.4. Gel Permeation Chromatography (GPC)

GPC was performed using a Waters 2695 instrument equipped with a refractive index detector. The conditions for the experiment are listed below. Samples were filtered with a 0.2 µm PTFE filter prior to injection. Data workup was performed using Waters Empower software. Molecular weights are relative to polystyrene standards (Polymer Standards Service PSKTR-4).

Column Set:	3 Mix-C and 1100 angstrom columns (PL gel, Agilent)
Mobile Phase:	Tetrahydrofuran
Flow rate:	1.0 mL/min
Column Temperature:	40°C
Injection Volume:	300 µL
RI Sensitivity:	16
RI Scale Factor:	20
Sample Concentration:	4 mg/mL
Sample Solvation Time:	6 hours

### 2.5. Kinematic Viscosity

Kinematic viscosity was determined by glass capillary viscometer where the temperature was maintained within 0.02°C [25] (Supplementary **Figures S2-S4**). The method utilized has a precision of 1% of the tested value. The kinematic viscosities of polymer solutions and a solvent ( $\nu$  and  $\nu_s$ , respectively) were used to calculate specific viscosities ( $\eta_{sp} = \nu/\nu_s - 1$ ).

**Table 1.** Molecular weight data for PAMA copolymers with a targeted degree of polymerization of 100.

Polymer	$M_n$ (kg/mol)	$M_w/M_n$	$C_\infty^a$	$\langle R^2 \rangle^{(1/2)}$ , nm
LMA	27.8	1.31	14.1	8
HMA:LMA	25.3	1.37	13.19	7.7
BMA:LMA	24.9	1.33	11.46 <sup>b</sup>	7.2
EMA:LMA	23.5	1.33	11.17	7.1
MMA:LMA	23.6	1.31	11.22	7.1

<sup>a</sup>Calculated using values for homopolymers from polymer data base [23]; <sup>b</sup>Calculated using value for homopolymer from Mays [24].

## 2.6. Viscosity Index

The VI of a fluid is a calculation to measure the variation in viscosity with respect to temperature. Defined by Dean and Davis in the 1920s and utilized by the petroleum lubrication industry since, viscosity index is an important measure of thermal effects on the viscous properties of the lubricating fluid [26]. To improve the overall efficacy of these oils, viscous properties of a fluid must be maintained over a wide range of temperatures. At lower temperatures, oils must maintain a low viscosity to permit oil pumping and cranking. At higher temperatures, oils must maintain a higher viscosity at to provide a full-film lubrication regime to protect parts from wear and prevent overheating. Although the lubrication industry eventually developed methods to determine viscosities at elevated and reduced temperatures [27] [28], the viscosity index continues to be a standard measure for a fluid's ability to meet certain performance criteria.

The standard practice for calculating VI was published by ASTM [29], where a kinematic viscosity (KV) method by glass capillary viscometer was utilized for the determination. VI is calculated using Equation (1)

$$VI = \left[ \frac{L-U}{L-H} \right] * 100 \quad (1)$$

where Covitch [30] identifies the variables in Equation (2) as:  $L$  is the calculated value of the 40°C KV of low VI reference fluid,  $H$  is the calculated value of the 100°C KV of the high VI reference fluid, and  $U$  is the measured value of the 40°C KV of the test fluid.

$$L = 0.8353Y^2 + 14.67Y - 216 \quad (2)$$

$$H = 0.1684Y^2 + 11.85Y - 97,$$

where  $Y$  is the measured value of the 100°C KV of the test oil.

Although other methods of calculation and discrepancies found at lower viscosities have been identified by Wright [31] and Zakarian [32] [33], the formulation space in which we are working permits that the standard calculation method is acceptable.

### Intrinsic Viscosity [ $\eta$ ] and Interaction Parameters ( $K_H$ and $K_M$ )

The intrinsic viscosity  $[\eta]$  has long been a method in polymer chemistry as identifying a polymer's effect on a solution's viscosity, specifically in the dilute regime where  $c < c^*$ , where  $c^*$  defined by Graessley is the boundary between the dilute and semi-dilute polymer regime or the critical overlap concentration [34]. Also,  $c^*$  has the basic relationship with intrinsic viscosity, Equation (3)

$$c^* = \frac{0.77}{[\eta]} \quad (3)$$

with units of inverse concentration, dL/g or mL/g, the intrinsic viscosity of a fluid represents the random-coil volume per unit mass that the polymer takes. This concept derives from the use of Einstein's relationship of non-interacting, non-deformable spheres to predict viscosity, Equation (4)

$$\eta_r = 1 + 2.5\phi \quad (4)$$

where  $\eta_r$  is the relative viscosity or ratio of solution viscosity to solvent viscosity and  $\phi$  which is the volume fraction of spheres [35].

Converting Einstein's relationship for the use in polymer applications to a virial expansion expression, Equation (5)

$$\eta_r = 1 + [\eta]c + k_H([\eta]c)^2 \quad (5)$$

From that expansion we can derive the Huggins Equation, Equation (6), which relates the reduced viscosity ( $\eta_{sp}/c$ ) to the concentration (g/dL), intrinsic viscosity (dL/g), and the Huggins parameter,  $k_H$ , which is related to the intramolecular interaction and solvent quality [36].

$$\frac{\eta_{sp}}{c} = [\eta] + k_H [\eta]^2 c \quad (6)$$

Determining the intrinsic viscosity requires dilution of a polymer system as limit of  $c$  goes to 0 g/dL,  $\lim_{c \rightarrow 0} \frac{\eta_{sp}}{c}$ , or the y-intercept  $\eta_{sp}/c$  vs.  $c$ , and  $k_H$  is determined by the slope of  $\eta_{sp}/c$  vs.  $c$ .

The poly(alkyl methacrylate) systems prepared herein, with solutions from 1 wt% to 5% at 1% increments, then at increasing increments to 25 wt% were prepared with the concentration being converted to g/dL for analysis. The concentrations provided an adequate number of solutions below  $c^*$  as well as samples above the expected overlap concentration.

Another method to calculate intrinsic viscosity with a corresponding interaction parameter is to use the Martin Equation, Equation (7), which provides a method to calculate the intrinsic viscosity with the inclusion of concentrations where  $c > c^*$

$$\frac{\eta_{sp}}{c} = [\eta] * \exp([\eta]K_M c) \quad (7)$$

where  $K_M$  is the Martin parameter. We found with our analysis of the data, where  $c \rightarrow c^*$  and beyond, the Martin equation is a more effective way of fitting the specific viscosity data.

### KRL Shear Stability Measurements

Using a KRL tapered roller bearing, approximately 40 mL of the test oil is heated to 60 °C and placed under a constant load of 5000 N with the roller bearing rotating at 1450 min<sup>-1</sup> for 20 hours. The KV100 is measured after the shear test and used to calculate the shear stability index. Further details of this method can be found in CEC L-45-A-99 [37].

### Shear Stability Index

The SSI is a measure of an oil's irreversible viscosity loss from shear of the viscosity modifier when the oil is subjected to engine operation, or specialized tests such as Sonic (ASTM D2603 or ASTM D5261), Orbahn (ASTM D6278 or ASTM D7109), or KRL (CEC L-45-99 Mod.) shear stability tests. The shear stability index of an oil is defined by Equation (8),

$$SSI = 100 * \left( \frac{V_0 - V_s}{V_0 - V_b} \right) \quad (8)$$

where  $V_0$  is the viscosity of the unsheared oil,  $V_s$  is the viscosity of the sheared oil, and  $V_b$  is the viscosity of the base oil.

Therefore, an SSI of 0 represents zero loss of oil viscosity due to polymer shear degradation, whereas an SSI of 100 indicates complete loss of the viscosity contribution from the viscosity modifier due to shearing.

## 3. Results and Discussion

The analysis of viscosity for dilute and semi-dilute solutions of copolymers can be used to understand the effect of side chain functionality (*i.e.*, alkyl chain length and branching) on the hydrodynamic properties of macromolecules and, consequently, viscosity index and the shear stability index. To examine these effects, five PAMAs with the same degree of polymerization were synthesized: LMA, HMA:LMA, BMA:LMA, EMA:LMA, and MMA:LMA. **Figure 1** shows

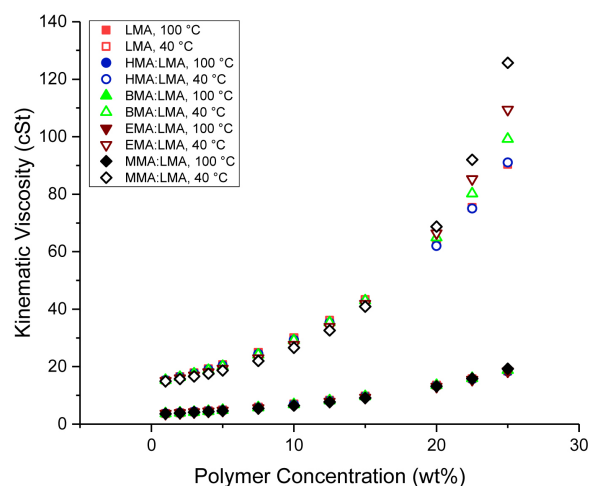


**Figure 1.** Kinematic viscosity at 40 °C and 100 °C as a function of polymer concentration. The KV100 values for all four PAMAs are nearly identical, while differences in KV40 values are noted across the concentration range studied.

the kinematic viscosity of PAMAs at polymer concentrations  $c$  ranging from 1 wt% to 25 wt% in a group III base oil. The closed and open symbols represent the kinematic viscosity measured at 100°C and 40°C, respectively. The results are quite similar across the set of PAMAs, especially at 100°C where the values are nearly identical. However, at 40°C, the differences in viscosity are quite significant, especially for polymer  $c > 20$  wt%.

The strong effect of chemical structure on viscosity at  $T = 40^\circ\text{C}$  can be understood in terms of inter-chain hydrodynamic interactions that become significant at high polymer concentrations. The viscosity of polymer solutions can be presented in the form:

$$\eta = \eta_s \left( 1 + [\eta]c + [\eta]^2 c^2 k_H + \dots \right) \quad (9)$$

Here,  $\eta_s$  is the solvent viscosity,  $[\eta]$  is intrinsic viscosity,  $c$  is polymer concentration, and  $k_H$  is the Huggins interaction constant. For the dilute regime ( $c/c^* = [\eta]c/0.77 \ll 1$ ), the polymer chains do not overlap and the contribution of polymer chains to the solution viscosity is due to hydrodynamic interactions. In the intermediate semi-dilute regime ( $c/c^* \leq 1$ ), the applicability of Equation (9) is limited to chains with strong excluded volume effect, *i.e.* when the hydrodynamic radius of macromolecules scales with the degree of polymerization as  $R_H \propto N^\nu$  with the excluded volume exponent  $\nu = 3/5$  for good solvents [11]. As the  $R_H$  and  $[\eta]$  are related through Flory-Fox expression

$$[\eta] \approx \Phi \frac{R_H^3}{M_n} \propto \frac{N^{3\nu-1}}{m} \quad (10)$$

here,  $\Phi$  is the universal Fox-Flory constant and  $m$  is the molecular weight of monomer unit. Equation (10) can support the coil-expansion theory if we assume that the excluded volume exponent increases with temperature. For the copolymers presented in this study, the temperature dependence  $[\eta]$  can be associated with increasing excluded volume exponent  $\nu$  due to increasing solubility of the side chains. Note that for  $\theta$ -solvents, where the repulsive interactions and van der Waals attractions between polymer segments cancel each other, the exponent  $\nu = 1/2$ . For prevailing van der Waals attractions, the coils may collapse so that  $1/3 < \nu < 1/2$  and the viscosity decreases due to small hydrodynamic radius,  $R_H$ . Therefore, the temperature dependencies of  $[\eta]$  can be used to characterize the effect of temperature on chain expansion for PAMAs presented in this paper.

The significant differences in the temperature dependence of  $[\eta]$  for PAMAs with the same degree of polymerization, but different side groups (**Figure 2**) demonstrate a large effect on molecular volume: very strong temperature dependence of  $[\eta]$  is observed for EMA:LMA and MMA:LMA copolymers whereas this dependence is relatively weak for homopolymer LMA and HMA:LMA copolymer. Incorporation of butyl side chains leads to an intermediate temperature dependence. The polymer coil volume depends on two factors: the characteristic ratio  $C_\infty$  that defines the flexibility of polymer molecules and the statistical coil size in solution (**Table 1**) and excluded volume effect that depends on

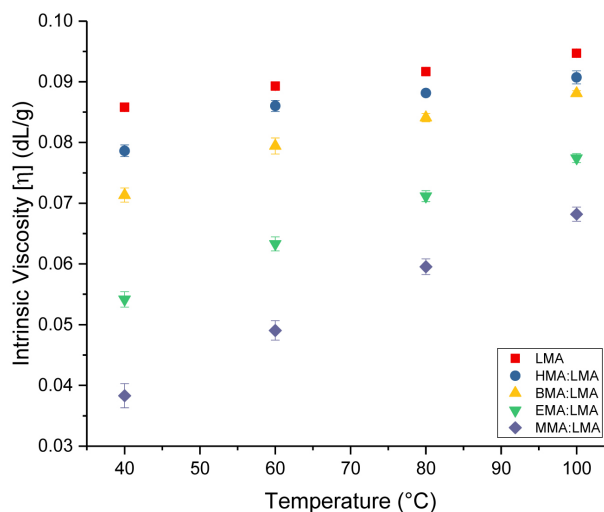


**Figure 2.** Intrinsic viscosity at various temperatures for poly (alkyl methacrylates). Error bars represent the standard error from the regression of the specific viscosity vs. concentration data to determine intrinsic viscosity.

solvent quality. This explains large difference between the values of  $[\eta] \propto R_H^3/M_w$  observed for LMA and MMA:LMA and EMA:LMA copolymers. The chains of copolymers are more flexible due to the smaller volume occupied by short MMA and EMA side chains as compared to the bulky LMA chains and, to a lesser degree, the HMA and BMA chains. This makes the polymer molecular size more sensitive to the excluded volume effects that become more significant at high temperature.

As the intrinsic viscosity reflects the behavior of isolated polymer chains, it is insufficient for quantitative interpretation of VI improvement for PAMAs. The hydrodynamic and even attractive inter-chain interactions may become dominant for higher concentrations ( $c \sim c^*$ ) and low temperatures. In the context of VI improvement, the polymer contribution to viscosity  $\eta_p = \eta - \eta_s$  due to inter-chain interactions must be described separately from the temperature dependence of polymer coil volume.

**Figure 3** shows the dependences of specific viscosity  $\eta_{sp} = \eta_p/\eta_s$  on  $c/c^*$  for  $T = 40^\circ\text{C}$  and  $100^\circ\text{C}$  for PAMAs. Remarkably, the value of  $\eta_{sp}$  for MMA:LMA and EMA:LMA copolymers steeply increases with  $c/c^*$  at  $T = 40^\circ\text{C}$  even when  $c/c^* \ll 1$ , which indicates that the polymer molecules behave similar to weakly attractive colloidal particles. At  $100^\circ\text{C}$ , this effect is observed in the more concentrated regime,  $c/c^* > 1$ , which suggests that at this temperature, PAMAs behave more like regular polymers.

For analyzing strong intermolecular interactions observed for PAMA copolymers, it is necessary to use the exponential dependence of  $\eta_{sp}$  vs.  $c$ , or Martin equation [38]:

$$\eta_{sp} = [\eta] c e^{K_M [\eta] c} \quad (11)$$

which reduces to Equation (9) for  $K_M [\eta] c \ll 1$ , *i.e.*  $K_M = k_H$ . The values of  $k_H$

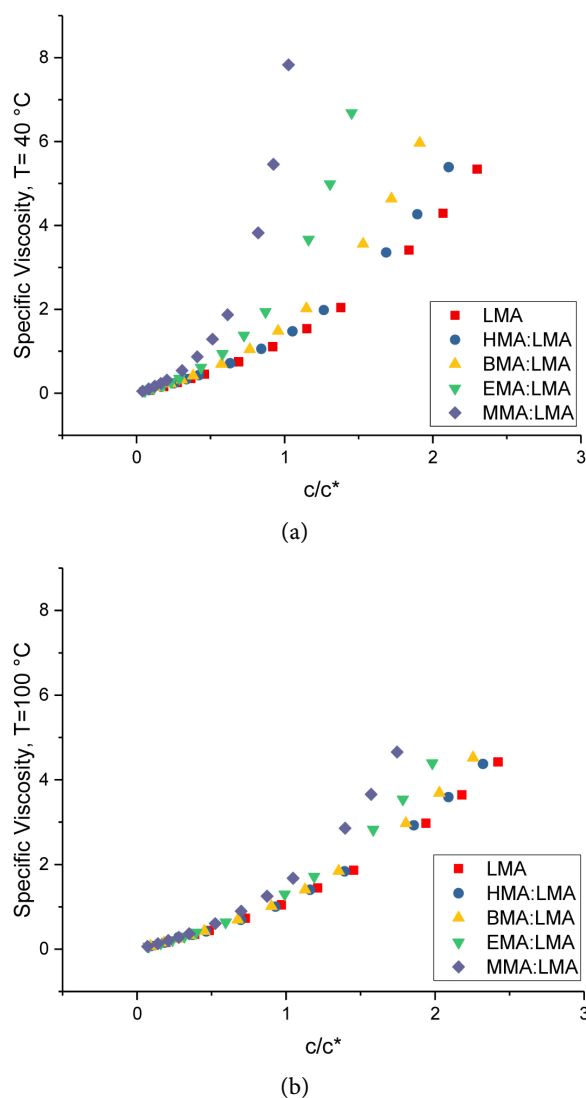


**Figure 3.** Specific viscosity vs.  $c/c^*$  at  $40^\circ\text{C}$  (a) and  $100^\circ\text{C}$  (b).

for good solvents are in the range of  $k_H = 0.3 - 0.4$  and for  $\theta$ -solvents  $k_H = 0.5 - 1.5$  [11], increasing with molecular weight. As PAMA copolymers have relatively low  $M_n$  (Table 1), the lowest range of  $K_H = 0.5$  is expected in  $\theta$ -solvents.

The values of  $K_M$  and  $[\eta]$  in Table 2 for PAMAs at  $T = 40^\circ\text{C}$  and  $100^\circ\text{C}$  demonstrate the drastic difference between LMA and HMA:LMA, and the copolymers with less soluble side chains (*i.e.*, BMA:LMA, EMA:LMA, and MMA:LMA). For LMA and HMA:LMA, the values of  $K_M$  are in the range

$K_M \sim 0.46 - 0.74$  at all temperatures, which is consistent with  $\theta$ -conditions. A small change in both  $K_M$  and  $[\eta]$  for these polymers suggests that coil expansion and intermolecular hydrodynamic interactions play less significant roles in VI control than for BMA:LMA, EMA:LMA, and MMA:LMA. For the latter, both  $K_M$  and  $[\eta]$  change significantly with temperature suggesting the possibility of controlling VI in the wider range.

**Table 2.** Intrinsic viscosity and Martin constants of poly(alkyl methacrylates) (DP = 100) at various temperatures in mineral oil.

Polymer or copolymer	Intrinsic Viscosity (dL/g)	40 °C	60 °C	80 °C	100 °C
LMA	$[\eta]$	0.0858	0.0893	0.0917	0.0946
	$K_M$	0.6225	0.5524	0.5094	0.4623
HMA:LMA	$[\eta]$	0.0786	0.0860	0.0882	0.0907
	$K_M$	0.7371	0.5823	0.5446	0.4998
BMA:LMA	$[\eta]$	0.0713	0.0794	0.0841	0.0881
	$K_M$	0.9472	0.7323	0.6265	0.5501
EMA:LMA	$[\eta]$	0.0542	0.0633	0.0712	0.0774
	$K_M$	1.5947	1.1341	0.8612	0.6913
MMA:LMA	$[\eta]$	0.0383	0.0491	0.0595	0.0682
	$K_M$	2.8869	1.8429	1.2474	0.9196

### Viscosity Index

The significant differences in the temperature dependence of  $[\eta]$  for PAMAs with the same degree of polymerization, but with different alkyl side chains, help explain the differences in VI measured for solutions of these copolymers at various concentrations. Indeed, the dependence of VI on concentration (**Figure 4**) demonstrates a significant variation in behavior based on the size of the alkyl group. The MMA:LMA and EMA:LMA copolymers exhibit a peak VI, after which increased polymer concentration results in a rapidly decreasing VI. Alternatively, the polymers containing monomers with longer side chains (*i.e.*, HMA:LMA copolymer and LMA homopolymer) show a VI plateau at a similar concentration. The BMA:LMA copolymer exhibits only a slight decrease in VI is observed past the maximum. These trends have also been identified and discussed by Willett, *et al.* [21]. A closer look at the concentration-dependence of the kinematic viscosities clearly shows the origin of this behavior. As shown in **Figure 1**, the kinematic viscosities at 100 °C are nearly identical for all PAMAs across the entire concentration range. However, distinct differences are noted in the measurements at 40 °C. A significant increase in low-temperature viscosity for MMA:LMA and EMA:LMA copolymers observed at polymer concentrations above 10% clearly contribute to this behavior.

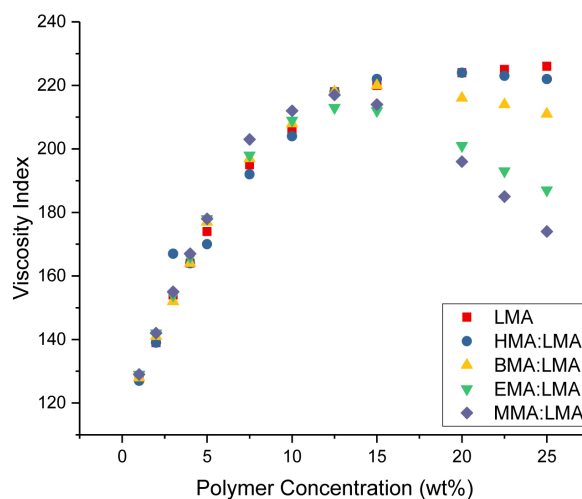


**Figure 4.** Viscosity index as a function of polymer concentration.

The effect of polymer concentration on VI can be explained in terms of the definition of VI (Equation (1)); the decrease in VI for high polymer concentration  $c$  is associated with the relatively strong effect of  $c$  on low-temperature viscosity as compared to that of high-temperature viscosity. This is consistent with a strong temperature dependence of the Martin constant for EMA:LMA and MMA:LMA copolymers (Table 2). To evaluate the effect of  $K_M$  on VI, we plot VI as a function of  $c/c^*$  for the two cases when  $c^*$  is estimated from the intrinsic viscosity values measured at  $T = 40^\circ\text{C}$  and  $100^\circ\text{C}$  as shown in Figure 5. The rationale for presenting the VI scaled with  $c/c^*$  for these temperatures is that the VI solely depends on viscosities measured at  $T = 40^\circ\text{C}$  and  $100^\circ\text{C}$ . This type of scaling helps to compare the concentration dependencies of VI for polymers in dilute and semi-dilute regimes defined by the value of  $c/c^*$ . In the dilute regime ( $c/c^* \ll 1$ ), the VI scales linearly with  $c/c^*$  for LMA homopolymer and HMA:LMA copolymer. The dependencies of VI on  $c/c^*$  almost collapse indicating that the VI for these polymers is dominated by the chain volume  $V_{ch} \propto 1/c^*$ . The value of VI reaches a plateau in the semi-dilute regime ( $c/c^* > 1$ ) for these polymers when  $c^*$  is estimated from  $[\eta]$  measured at  $40^\circ\text{C}$  and  $100^\circ\text{C}$ . Conversely, the VI reaches a maximum at  $c/c^* \sim 0.5$  for MMA:LMA and  $c/c^* \sim 0.7$  for EMA:LMA copolymers. These dependencies do not collapse even when  $c/c^* < 0.5$ . This effect is also seen to a lesser extent in the BMA:LMA copolymer. For these polymers, the viscosity index is controlled not only by the chain volume but also by the hydrodynamic and attractive interactions between the chains. This effect is more pronounced when the value of  $c^*$  is estimated from  $[\eta]$  measured at  $T = 40^\circ\text{C}$ , which is related to the strong temperature dependence of Martin constants for these polymers (Table 2).

To further understand the correlation between VI, the chemical structure of copolymers, and their associated rheological characteristics, we can shift the dependences of VI on  $c/c^*$  using horizontal shift factor  $a_k$  and relate the values of  $a_k$  and  $K_M$  for each polymer at a given temperature.

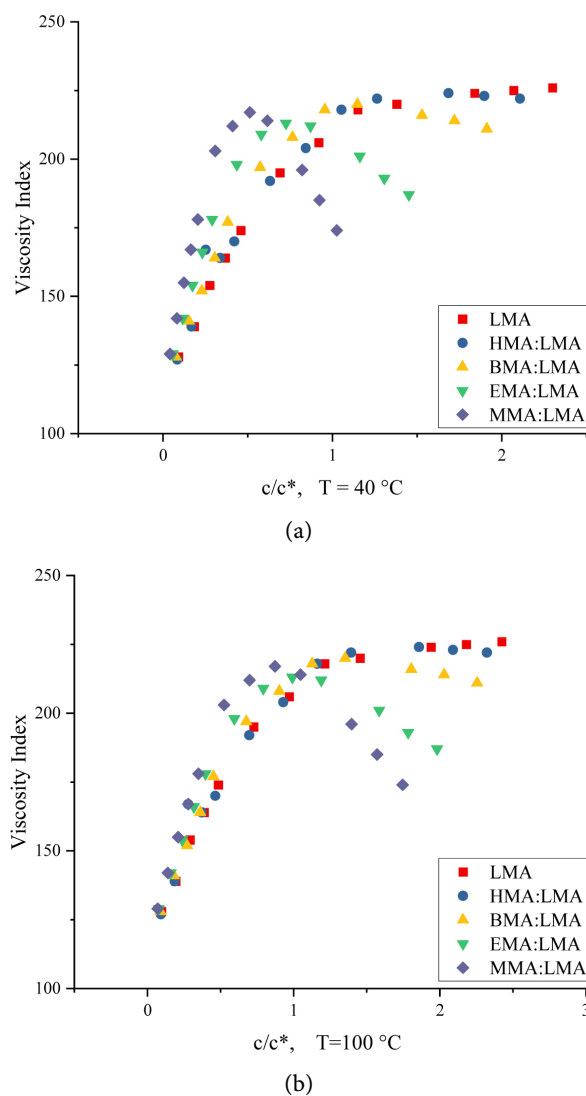


**Figure 5.** Viscosity index vs.  $c/c^*$  at  $40^\circ\text{C}$  (a) and  $100^\circ\text{C}$  (b).

**Figure 6** shows the shifted dependencies of VI at  $40^\circ\text{C}$  and  $100^\circ\text{C}$  as a function of  $a_k(c/c^*)$  with the values of  $c^*$  determined from  $[\eta]$  at  $T = 40^\circ\text{C}$  and  $100^\circ\text{C}$ , respectively. The insets demonstrate the relationships between the shift factors  $a_k$  and the Martin constants  $K_M$ . Interestingly, the dependences of VI on  $a_k(c/c^*)$  scale together for  $a_k(c/c^*) < 1$  but diverge for higher concentrations when the interactions between polymer chains become dominant. For copolymers containing less-soluble monomers (MMA:LMA and EMA:LMA), the enhanced intermolecular interactions at  $T = 40^\circ\text{C}$  help to increase the VI as compared to those with HMA:LMA and LMA. However, very same interactions reduce the VI at higher polymer concentrations. As noted in previous analyses, the BMA:LMA copolymer displays behavior intermediate to the other copolymers.

#### Shear stability

Another technologically important parameter is shear stability, or the resistance of macromolecules to mechanical degradation caused by shear forces.

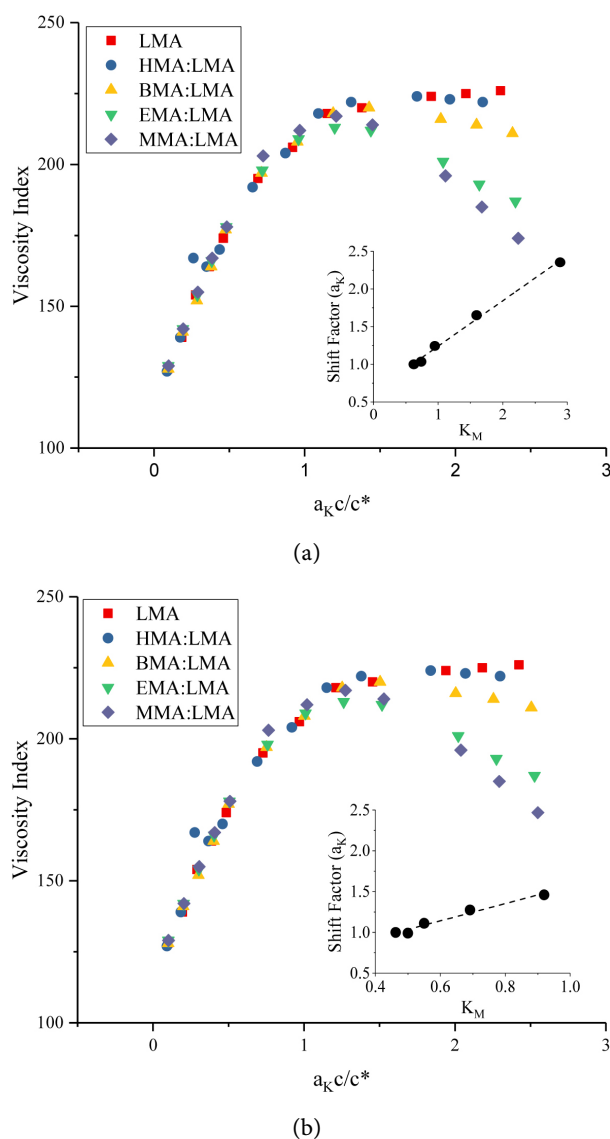


**Figure 6.** Viscosity Index vs.  $a_K c/c^*$  at 40°C (a) and 100°C (b). The insets show the dependencies of horizontal shift factors  $a_K$  on the Martin constant  $K_M$

This parameter is inherently linked to macromolecule size as larger macromolecules are more susceptible to shear degradation. Since all polymers studied in this work have nearly identical degrees of polymerization, it is assumed that their contour lengths are also quite similar. Therefore, any differences in shear stability are attributed to changes in the hydrodynamic coil size  $R_H \propto N^\nu$ . The exponent  $a = 3\nu - 1$  in the Mark-Houwink equation  $[\eta] = KM^a$  can be used to characterize the quality of solvent and the coil size in solution. To evaluate these parameters, well-defined polymers of LMA and MMA:LMA with higher degrees of polymerization (target DP = 200 and 400) were synthesized (Supplementary Figure S5 and Figure S6, and Supplementary Table S1). At 100°C, values of  $a = 0.779$  and  $\nu = 0.593$  were measured for LMA, indicating that mineral oil is a “good” solvent for LMA. At 40°C, these parameters are slightly

lower but still within the range found for good solvents. The high solubility of LMA was expected due to the oleophilic nature of the lauryl side chains which dominates over the more hydrophilic methacrylate moieties of the polymer. Alternately, the copolymer of MMA:LMA exhibits much lower solubility, with  $\alpha = 0.61$  and  $0.53$  and  $\nu = 0.536$  and  $0.510$  determined at  $100^\circ\text{C}$  and  $40^\circ\text{C}$ , respectively. When the lauryl side chains are replaced with shorter methyl groups, the dominating factor of the oleophilic lauryl groups is diminished, thus increasing the hydrophilicity of the overall polymer. This results in poorer solvent quality, which is magnified as the solution temperature is cooled. As the value of  $a$  decreases for MMA:LMA copolymer as compared to LMA homopolymer (Table 3), the former polymer is expected to be more resistant to shear degradation than the latter.

The shear stability of LMA and MMA:LMA polymers was examined using the KRL shear stability test at various solution viscosities (*i.e.*, multiple polymer concentrations). At similar KV100, the MMA:LMA copolymers are noticeably more shear stable than the LMA homopolymer (Figure 7). As mentioned previously, this difference is explained by the different sizes of macromolecules in solution; at  $60^\circ\text{C}$  (the measurement temperature), the LMA homopolymer is significantly more soluble than the MMA:LMA copolymer, and therefore is more extended and more susceptible to cleavage events. The relationship between the solubility and the polymer coil size has been outlined by Rubenstein (11); briefly, the excluded volume  $\nu = (1 - 2\chi)b^3$ , where  $b$  is the size of monomer unit,  $\chi$  is the Flory-Huggins parameter characterizing the polymer-solvent interactions. The value  $\chi$  is related to the solubility parameters of polymer segment and solvent molecules. For  $\theta$ -solvents,  $\chi = 1/2$ ,  $\nu = 0$ , and the coil size is  $R_H \propto N^{1/2}$ . For good solvents with  $\chi < 1/2$ , the excluded volume  $\nu > 0$  and  $R_H \propto N^{3/5}$ . Therefore, the side chain length (and more specifically the polymer solubility) directly impacts the shear stability of a macromolecule.

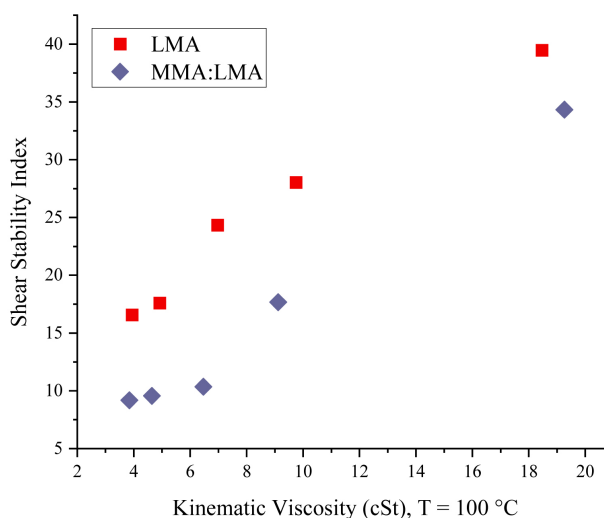


**Figure 7.** Shear stability index as a function of kinematic viscosity at  $100^\circ\text{C}$  for LMA homopolymer and MMA:LMA copolymer.

**Table 3.** Mark-Houwink parameters for LMA and MMA:LMA at various temperatures in mineral oil.

Polymer or copolymer	Mark-Houwink	40°C	100°C
LMA $M_w$ range: ~30 k - 150 k	$K$	0.355E-04	0.265E-04
	$\alpha$	0.742	0.779
	$\nu$	0.581	0.593
MMA:LMA $M_w$ range: ~30 k - 100 k	$K$	1.51E-04	1.25E-04
	$\alpha$	0.529	0.607
	$\nu$	0.510	0.536

## 4. Conclusion

A series of PAMAs were synthesized by RAFT polymerization to study the effect of the alkyl side chain length on the ability of a PAMA to control viscosity index and shear stability in mineral oil solutions over a wide concentration range. The major goal of this study was to understand the role of the intrinsic viscosity  $[\eta]$  and the Huggins or Martin constants ( $k_H$  or  $K_M$ ) in controlling the viscosity index of polymer solutions analyzing temperature and concentration dependences of  $[\eta]$  and  $K_M$ . The VI for all polymer solutions was presented as a function of  $a_k c/c^*$  where  $a_k$  is the scaling factor that is related to the Martin constant. This scaling allows one to separate the contribution of molecular size and the intermolecular interactions by means of reduced concentration  $c/c^*$  and scaling factor  $a_k$ , respectively. The master curve of VI vs.  $a_k c/c^*$  can be used for all polymers in this study to formulate the oil with desirable VI characteristics within the practically important range of concentrations, *i.e.*,  $c/c^* < 1$ . It was also shown that an LMA homopolymer has much higher SSI values (lower shear stability) as compared to an MMA:LMA copolymer over a wide range of kinematic viscosities (or polymer concentrations). These results directly relate the shear stability of the macromolecules to the polymer coil size, which is dictated by polymer solubility and ultimately side-chain characteristics.

## Conflicts of Interest

The authors declare no conflicts of interest regarding the publication of this paper.

## References

- [1] Stribeck, R. (1901) Kugellager für beliebige Belastungen [Ball Bearings for Any Stress]. *Zeitschrift des Vereins Deutscher Ingenieure*, **45**.
- [2] Hersey, M.D. (1914) The Laws of Lubrication of Horizontal Journal Bearings. *Journal of the Washington Academy of Sciences*, **4**, 542-552.
- [3] Umamori, N. and Kugimiya, T. (2003) Study of Viscosity Index Improver for Fuel Economy ATF. SAE Technical Paper 2003-01-3256. <https://doi.org/10.4271/2003-01-3256>

- [4] Vickerman, R., Streck, K., Schiferl, E., and Gajanayake, A. (2010) The Effect of Viscosity Index on the Efficiency of Transmission Lubricants. *SAE International Journal of Fuels and Lubricants*, **2**, 20-26. <https://doi.org/10.4271/2009-01-2632>
- [5] Lauterwasser, F., Bartels, T., Smolenski, D., and Seemann, M. (2016) Megatrend Fuel Economy: How to Optimize Viscosity with VI Improvers. SAE Technical Paper 2016-28-0030. <https://doi.org/10.4271/2016-28-0030>
- [6] Clevenger, J., Carlson, D., and Kleiser, W. (1984) The Effects of Engine Oil Viscosity and Composition on Fuel Efficiency. SAE Technical Paper 841389. <https://doi.org/10.4271/841389>
- [7] Selby, T.W. (1958) The Non-Newtonian Characteristics of Lubricating Oils. *ASLE Transactions*, **1**, 68-81. <https://doi.org/10.1080/05698195808972315>
- [8] Dean, E.W. and Davis, G.H.B. (1929) Viscosity Variation of Oils with Temperature. *Chemical and Metallurgical Engineering*, **36**, 618-619.
- [9] Walther, C. (1933) Evaluating Lubricating Oils. *Oel und Kohle*, **1**, 71-74.
- [10] Covitch, M.J. and Trickett, K.J. (2015) How Polymers Behave as Viscosity Index Improvers in Lubricating Oils. *Advances in Chemical Engineering and Science*, **5**, 134-151. <https://doi.org/10.4236/aces.2015.52015>
- [11] Rubinstein, M and Colby, R. (2003) *Polymer Physics*. Oxford University Press, Oxford.
- [12] Kulicke, W.M. and Clasen, C. (2004) Determination of the Polymer Coil Dimensions from the Intrinsic Viscosity. In: Kulicke, W.M. and Clasen, C., Eds., *Viscosimetry of Polymers and Polyelectrolytes*, Springer, Berlin, 91-94. [https://doi.org/10.1007/978-3-662-10796-6\\_7](https://doi.org/10.1007/978-3-662-10796-6_7)
- [13] Lutz, J.F., Weichenhan, K., Akdemir, O. and Hoth, A. (2007) About the Phase Transitions in Aqueous Solutions of Thermoresponsive Copolymers and Hydrogels Based on 2-(2-Methoxyethoxy)ethyl Methacrylate and Oligo(Ethylene Glycol) Methacrylate. *Macromolecules*, **40**, 2503-2508.
- [14] Kayaman, N., Gurek, E.E., Baysal, B.M., and Karasz, F.E. (2000) Coil to Globule Transition Behaviour of Poly(Methyl Methacrylate) in Isoamyl Acetate. *Polymer*, **41**, 1461-1468. [https://doi.org/10.1016/S0032-3861\(99\)00316-X](https://doi.org/10.1016/S0032-3861(99)00316-X)
- [15] Stickler, M., Panke, D., and Wunderlich, W. (2003) Solution Properties of Poly(Methyl Methacrylate) in Methyl Methacrylate. Viscosities from the Dilute to the Concentrated Solution Regime. *Die Makromolekulare Chemie*, **188**, 2651-2664. <https://doi.org/10.1002/macp.1987.021881116>
- [16] Hernandez-Fuentes, I., *et al.* (1982) Limits of the Dilute Regime for the Solution Viscosity of PMMA in Good and in Poor Solvents. *European Polymer Journal*, **18**, 29-35. [https://doi.org/10.1016/0014-3057\(82\)90128-8](https://doi.org/10.1016/0014-3057(82)90128-8)
- [17] Lenka, S., Nayak, P.L., and Dash, M. (1983) Solution Properties of Poly(Methyl Methacrylate) by Viscometric Measurements in Organic Solvents. I. *Journal of Macromolecular Science. Part A—Chemistry*, **20**, 469-486. <https://doi.org/10.1080/00222338308060795>
- [18] Chinai, S.N., Matlack, J.D., Resnick, A.L. and Samuels, R.J. (1955) Polymethyl Methacrylate: Dilute Solution Properties by Viscosity and Light Scattering. *Journal of Polymer Science*, **17**, 391-401. <https://doi.org/10.1002/pol.1955.120178507>
- [19] Lal, J. and Green, R. (1956) Intrinsic Viscosities and Polymerization Speeds in Methacrylic Ester-Alkyl Polymethacrylate Systems. *Journal of Polymer Science*, **20**, 387-396. <https://doi.org/10.1002/pol.1956.120209514>
- [20] Ramasamy, U.S., Lichter, S., and Martini, A. (2016) Effect of Molecular-Scale Fea-

- tures on the Polymer Coil Size of Model Viscosity Index Improvers. *Tribology Letters*, **62**, 1-7.
- [21] Willett, E., DeVore, A., and Vargo, D. (2019) Viscometric and Low Temperature Behavior of Lubricants with Blended VI Improvers. *NLGI Spokesman*, **83**, 6-21.
- [22] Chiefari, Y.K., *et al.* (1998) Living Free-Radical Polymerization by Reversible Addition-Fragmentation Chain Transfer: The RAFT Process. *Macromolecules*, **31**, 5559-5562.
- [23] Crow Polymer Science. Polymer Properties Database. <https://polymerdatabase.com/polymer%20physics/C%20Table%20.html>
- [24] Mays, J.W. and Hadjichristidis, N. (1988) Characteristic Ratios of Polymethacrylates. *Journal of Macromolecular Science, Part C*, **28**, 371-401. <https://doi.org/10.1080/15583728808085380>
- [25] ASTM D445-21 (2021) Standard Test Method for Kinematic Viscosity of Transparent and Opaque Liquids (and Calculation of Dynamic Viscosity). ASTM International, West Conshohocken, PA. <https://www.astm.org/>
- [26] API 1509-19 (2019) API 1509 Annex E-API Base Oil Interchangeability Guidelines for Passenger Car Motor Oils and Diesel Engine Oils. <https://www.api.org/~media/Files/Certification/Engine-Oil-Diesel/Publications/AnnE-REV-09-20-19.pdf>
- [27] Spearot, J.A. (Ed.) (1989) High-Temperature, High-Shear (HTHS) Oil Viscosity: Measurement and Relationship to Engine Operation. American Society for Testing and Materials, STP1068-EB. <https://doi.org/10.1520/STP1068-EB>
- [28] Rhodes, R.B. (Ed.) (1992) Low Temperature Lubricant Rheology Measurement and Relevance to Engine Operation. American Society for Testing and Materials, STP1143-EB. <https://doi.org/10.1520/STP1143-EB>
- [29] ASTM D2270-10 (2016) Standard Practice for Calculating Viscosity Index from Kinematic Viscosity at 40 °C and 100 °C. ASTM International, West Conshohocken, PA. <https://www.astm.org/>
- [30] Covitch, M.J. (2018) An Improved Method for Calculating Viscosity Index (VI) of Low Viscosity Base Oils. *Journal of Testing and Evaluation*, **46**, 820-825. <https://doi.org/10.1520/JTE20150242>
- [31] Wright, W.A. (1964) A Proposed Modification of the ASTM Viscosity Index. *Proceedings of the American Petroleum Institute*, **44**, 535-541.
- [32] Zakarian, J.A. (2012) The Limitations of the Viscosity Index and Proposals for Other Methods to Rate Viscosity-Temperature Behavior of Lubricating Oils. *SAE International Journal of Fuels and Lubricants*, **5**, No. 3, 1123-1131.
- [33] Zakarian, J.A. (2013) V.I. Too Resistant to Change? Lubes 'n' Greases, 54-62.
- [34] Graessley, W.W. (1980) Polymer Chain Dimensions and the Dependence of Viscoelastic Properties on the Concentration, Molecular Weight and Solvent Power. *Polymer*, **21**, 258-262. [https://doi.org/10.1016/0032-3861\(80\)90266-9](https://doi.org/10.1016/0032-3861(80)90266-9)
- [35] Einstein, A. (1911) Eine Neue Bestimmung der Molekuldimensionen. *Annalen der Physik*, **339**, 591-592. <https://doi.org/10.1002/andp.19113390313>
- [36] Kumar, A. and Gupta, R.K. (1998) Fundamentals of Polymers. McGraw-Hill, New York.
- [37] CEC L-45-A-99 (1999) Viscosity Shear Stability of Transmission Lubricants (Taper Roller Bearing Rig). Brussels.
- [38] Matsuoka, S. and Cowman, M.K. (2002) Equation of State for Polymer Solution. *Polymer*, **43**, 3447-3453. [https://doi.org/10.1016/S0032-3861\(02\)00157-X](https://doi.org/10.1016/S0032-3861(02)00157-X)

## Supplementary Section

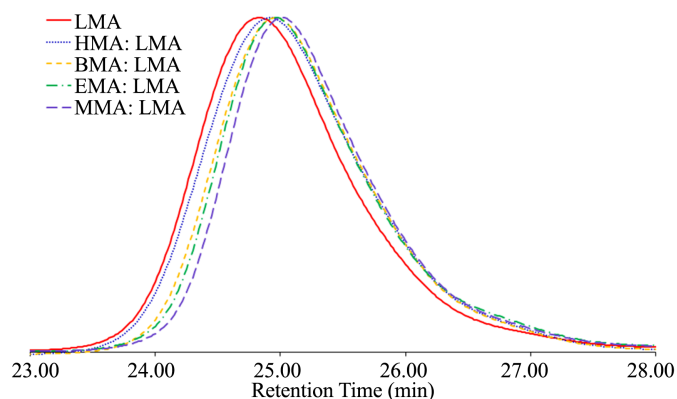


**Figure S1.** Gel permeation chromatograms of polymers with a targeted degree of polymerization of 100. LMA (blue), EHMA:LMA (red, dotted), EMA:LMA (green, dashed), and MMA:LMA (purple, dashed/dotted) all elute at similar times, supporting that they are of similar hydrodynamic volume.

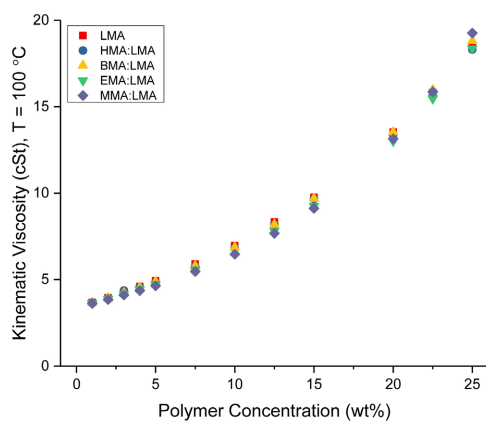


**Figure S2.** Kinematic viscosity at 100 °C as a function of concentration for LMA, HMA:LMA, BMA:LMA, EMA:LMA, and MMA:LMA. Very little difference in the viscosities of the various PAMAs is noted at 100 °C.

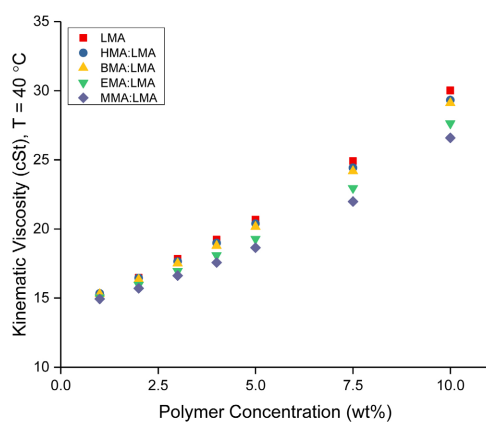


**Figure S3.** Kinematic viscosity at 40 °C at low polymer concentrations. Under these conditions, PAMAs containing MMA and EMA have lower kinematic viscosities, leading to a boost in viscosity index.

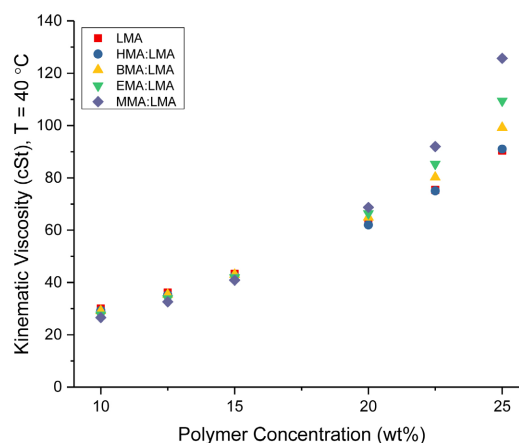


**Figure S4.** Kinematic viscosity at 40°C at high polymer concentration. At this point, intermolecular interactions begin to dominate and the PAMAs containing MMA and EMA have higher viscosities than the other polymers, leading to a downturn in viscosity index.

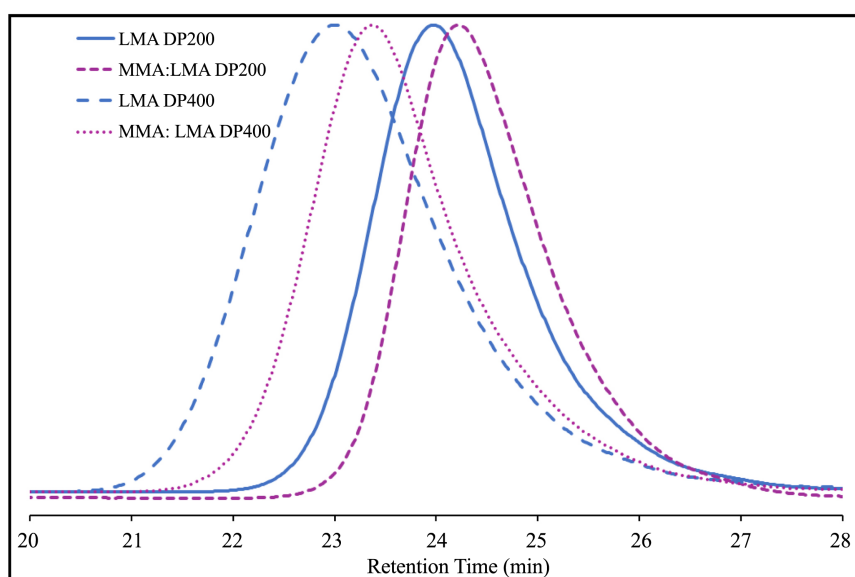
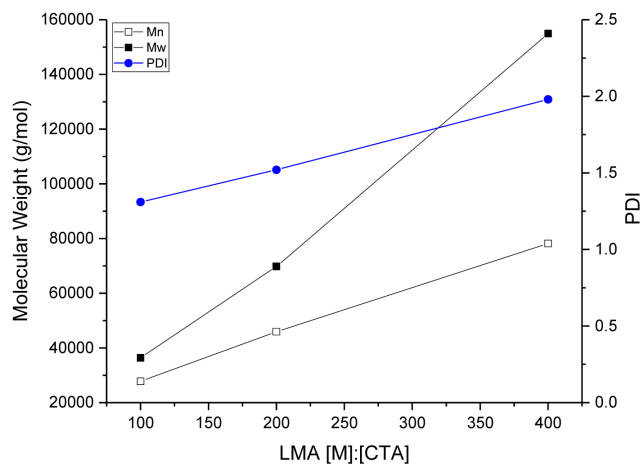


**Figure S5.** Gel permeation chromatograms of polymers with degrees of polymerization of 200 and 400. These polymers were prepared to evaluate the Mark-Houwink-Sakurada parameters for poly(lauryl methacrylate) and a copolymer of 52 mol% lauryl methacrylate and 48 mol% methyl methacrylate.

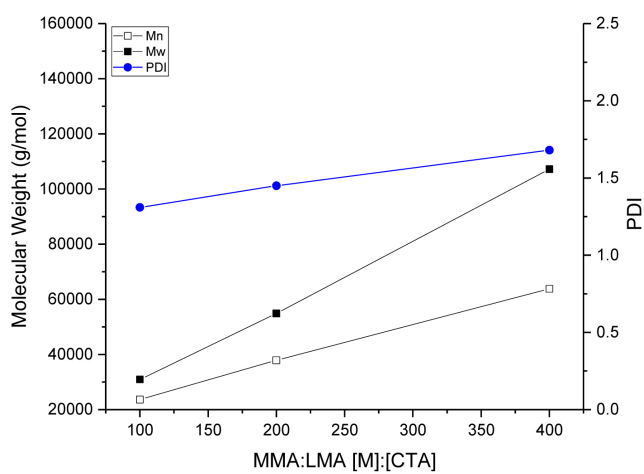
**Table S1.** Summary of GPC data for LMA and MMA:LMA polymers with targeted degrees of polymerization of 200 and 400.

Polymer	Target DP <sub>n</sub> <sup>a</sup>	$M_n$ (kg/mol) <sup>b</sup>	$M_w/M_n$ <sup>b</sup>	DP <sub>n</sub> <sup>b</sup>
LMA	200	45.9	1.52	181
	400	78.2	1.98	308
MMA:LMA	200	37.9	1.45	211
	400	63.8	1.68	354

<sup>a</sup>Calculated from initial ratio of  $[M]_0/[CTA]_0$ ; <sup>b</sup>From GPC analysis with polystyrene standards.



(a)



(b)

**Figure S6.** Molecular weight and dispersity data at targeted degrees of polymerization of 100, 200, and 400 for (a) LMA and (b) MMA:LMA.